UDC 004.942:537.525
DOI: 10.20535/SRIT.2308-8893.2024.4.11

AN ADVANCED METHOD OF INTERPOLATION OF SHORT-FOCUS ELECTRON BEAMS BOUNDARY TRAJECTORIES USING HIGHER-ORDER ROOT-POLYNOMIAL FUNCTIONS AND ITS COMPARATIVE STUDY

I. MELNYK, A. POCHYNOK, M. SKRYPKA

Abstract. The comparison of three advanced novel methods for estimating the boundary trajectory of electron beams propagated in ionized gas, including lower-order interpolation, self-connected interpolation, and extrapolation, as well as higher-order interpolation, is considered and discussed in the article. All estimations of the corresponding errors have been provided relative to numerically solving the set of algebra-differential equations that describe the boundary trajectory of the electron beam. By providing analysis, it is shown and proven that lower-order interpolation usually gives the minimal value of average error, using the method of self-connected interpolation and extrapolation gives the minimal error for estimation of focal beam parameters, and higher-order interpolation is suitable to obtain a uniform error value over the entire interpolation interval. All results of error estimation were obtained using original computer software written in Python.

Keywords: interpolation, extrapolation, lower-order interpolation, higher-order interpolation, root-polynomial function, ravine function, average error, electron beam, boundary trajectory, high voltage glow discharge, electron beam technologies.

INTRODUCTION

Interpolation of boundary trajectories of electron beams is very important task today, taking into account the high level of development electron beam technologies and its applying in modern industry [1–9].

Really, industrial electron-beam technologies have been developed and widely applied in industry since 60–70-th years of XX century [6–9], but its application in modern industry is also continued. Therefore, adaptation of traditional electron-beam technologies to corresponded advanced technological processes is successfully provided today [1–5; 10–13].

Today main branches of industry, where electron beam technologies find high level of application, are follows: metallurgy, mechanical engineering, electrical engineering, instrument making, microelectronic production, automotive, aircraft, and space industries [1–5].

For example, in microelectronic production point-focus electron beams with focal beam radius can be successfully applied for making contacts in precision cryogenic devices [14; 15]. Corresponded estimation of diameter of welding seam in electron-beam technologies have been provided recently in the paper [16; 17]. Other advanced application of electron-beam technologies in microelectronic production is refining of silicon [10–13] and obtaining of chemically-complex

ceramic films for high quality capacitors and for microwave transmitters and receivers in advanced communication systems [18–20]. Generally, advanced possibility of using electron beam technologies in modern microelectronic production are described in manual book [5].

In metallurgy advanced electron-beam technologies are widely used, since 60-years of XX century, for refining of refractory metals [21–23] and other refractory materials, in particular silicon for the microelectronics industry [11–13]. Among other, advanced application of electron beam heating in metallurgy, which have been developed in last few years, three-dimensional printing by the metals, including forming of details with complex spatial shape for aircraft and space industry, have to be mentioned and considered [24–26].

In energetic industry and electric vehicle production electron beam technologies are widely used for deposition high-quality ceramic insulator films [27–30]. Other advanced application of high-quality chemically-complex ceramic films in automotive, aircraft and space industry is obtaining heat-resistant and heat-protective thick films for details of engines, which operated under conditions of high temperature. For deposition such kind of films advanced method of physical vapor deposition by electron-beam heating is usually applied [27–30].

Special issue is applying of high-energy intensive electron beams, obtained in the accelerators, for changing the properties of treated materials. Corresponded technologies are described in the works [4; 31–33].

The advantages of electron beams, which caused its wide application in modern industrial technologies, are as follows [1–5].

1. High total power and power density in beam focus.

2. High energetic efficiency of electron beam sources.

3. Simplicity of fast control of beam power and spatial position of beam focus using electric and magnetic fields.

4. Wide range of different technological operations, which can be realized by electron beam heating and chemical treatment.

Taking into account pointed out advantages of electron beam technologies, elaboration of advanced improving industrial constructions of electron beam sources, which are called electron guns, is important scientific and engineering task today. Usually, this task solving using two different ways, which are, generally, follows.

1. Improving the constructions of electron guns with heated cathode, operated in conditions of high vacuum. Such kind of electron guns are traditional and widely use since 60–70-th years of XX century [6–9].

2. Elaboration of novel types of electron guns, based on auto-electronic emission of electrons in the string electric fields, photoemission, as well as on emission in gas discharges. Among this types of guns special place occupied high-voltage glow discharge electron guns, which particularities of operation will be considered in next part of this paper.

HIGH VOLTAGE GLOW DISCHARGE ELECTRON GUNS AND ADVANTAGES ITS APPLYING IN ELECTRON BEAM TECHNOLOGIES

In the last few decades, in some technological processes that are implemented in a soft vacuum in an environment of air or active gases, instead of the traditionally used guns with a heated cathode, alternative guns have been successfully applied, the operation of which is based on the use of a high-voltage glow discharge (HVGD). From a physical point of view, HVGD is considered a kind of dis-

charge, taking place under voltage between electrodes 5–40 kV and pressure in the discharge volume range of 0.1–10 Pa [34–36]. In the work [34–36] the basic principles of simulation HVGD electron guns have been considered, and corresponding mathematical relations were also given and analyzed. In the papers [37; 38] main advantages of applying HVGD electron guns for welding, melting processes, as well as for deposition of ceramic films have been pointed out. These advantages are as follows [37; 38].

1. High stability of operation in conditions of soft vacuum.
2. Relative simplicity of gun construction.
3. Relative simplicity of evacuation equipment for obtaining soft vacuum.
4. Since the current density from the cold cathode in HVGD conditions is not so large, range of 0.01 A/cm^2, using of enlarges cathode surface and suitable self-maintained electron-ion optics allows forming profile electron beams with linear and ring-like focus [37; 38].
5. Simplicity of control of gun current, both by relatively slow aerodynamic method using electromagnetic valve [39], and by fast electric method with lighting of low-voltage additional discharge in anode plasma region [40].
6. Possibility of providing operation of HVGD electron guns in impulse regime with obtaining advanced technological possibilities of pulsed electron beams [41–43].

The regulation time for slow electrodynamic control systems was estimated in the paper [39], and for fast electric control systems correspondently, in papers [41; 43].

However, simulation of HVGD electron guns is realized today mostly by solving of complex algebra-differential equations, described forming and interaction of charged particles flows in the soft vacuum conditions. The main problem in this task is defining of anode plasma boundary form and position. It caused by the fact, that in HVGD anode plasma is considered as the source of ions and as electrode with fixed potential, which is transparent to beam electrons [34–36]. Simplified analytical models for defining of focal beam parameters in HVGD aren't existed [34]. But namely such approximative estimations are very important for defining the technological possibilities of electron beams, especially on the first stage of gun designing [16; 17]. Absence of such simple approach of analytical calculations of focal beam parameters significantly hinders development and implementation in industry of HVGD electron guns, which advantages have been described above. Also using of sophisticated numerical calculation methods is lead to increasing the complexity of solving simulation problems in case of implementing cloud computing. Corresponded estimations have been given in works [44–46]. Therefore, finding the corresponding analytical relations for estimation focal parameters of electron beams, formed by HVGD electron guns, is very important scientific and engineering task today. This task will be considered in the next section of the article.

GENERAL STATEMENT OF PROBLEM OF INTERPOLATION BOUNDARY TRAJECTORY OF ELECTRON BEAM, PROPAGATED IN IONIZED GAS, AND ESTIMATION OF ERRORS

Firstly, the basic approach to interpolation the boundary trajectories of electron beams have been proposed in the years 2019–2020 in the papers [17; 47–49]. Generally, this approach is based on the following presumptions.

1. Numerical solving of basic set of algebra-differential equations for the boundary trajectory of short-focus electron beam, propagated in the soft vacuum conditions in the medium of ionized gas, which is, in general form, written as follows [1–6; 34; 49]:

$$f = \frac{n_e}{n_{i0} - n_e};\ C = \frac{I_b(1 - f - \beta^2)}{4\pi\varepsilon_0\sqrt{\frac{2e}{m_e}}U_{ac}^{1.5}};\ \frac{d^2 r_b}{dz^2} = \frac{C}{r_b};\ \theta = \frac{dr_b}{dz} + \theta_s;$$

$$n_e = \frac{I_b}{\pi r_b^2};\ v_e = \sqrt{\frac{2eU_{ac}}{m_e}};\ n_{i0} = r_b^2 B_i p n_e \sqrt{\frac{\pi M_i \varepsilon_0 n_e}{m_e U_{ac}}} \exp\left(-\frac{U_{ac}}{\varepsilon_0 n_e r_b^2}\right); \quad (1)$$

$$\gamma = \sqrt{1-\beta^2};\ \tan\left(\frac{\theta_{\min}}{2}\right) = \frac{10^{-4} Z_a^{4/3}}{2\gamma\beta^2};\ \tan\left(\frac{\theta_{\max}}{2}\right) = \frac{Z_a^{3/2}}{2\gamma\beta^2};$$

$$\overline{\theta}^2 = \frac{8\pi(r_b Z_a)^2 dz}{n_e} \ln\left(\frac{\theta_{\min}}{\theta_{\max}}\right),\ \beta = \frac{v_e}{c},$$

where U_{ac} is the voltage of HVGD lighting; I_b is the current of electron beam; p is the residual gas pressure in the volume of HVGD lighting; z is the longitudinal coordinate; r_b is the radius of the boundary trajectory of the electron beam; dz is the length of the electron path in the longitudinal direction at the current iteration; n_{i0} is the concentration of residual gas ions on the beam symmetry axis; n_e is the concentration of beam electrons'; v_e is the average velocity of the beam electrons; $\theta_{\min}$ and $\theta_{\max}$ are the minimum and maximum scattering angles of the beam electrons, corresponding to Rutherford model [1–6]; $\overline{\theta}$ $\theta_{\min}$ $\theta_{\min}$ is the average scattering angle of the beam electrons; f is the residual level of gas ionization; B_i is the gas ionization level; m_e is the electron mass; ε_0 is the dielectric constant; c is the light velocity; γ is the relativistic factor; M_i is the molecular mass of residual gas atoms, and Z_a is its' nuclear charge.

2. Choosing of k basic points (r_b, z) on the calculated boundary trajectory.

3. Interpolation of defined function $r_b(z)$ using ravine root-polynomial function [47–49]:

$$r_b(z) = \sqrt[n]{C_n z^n + C_{n-1} z^{n-1} + \ldots + C_1 z + C_0}, \quad (2)$$

where $n = k - 1$ is the degree of the polynomial and the order of the root-polynomial function, and $C_0, \ldots, C_n$ are the polynomial coefficients.

4. Defining of interpolation error using relation [47–49]:

$$\varepsilon(\mathrm{z}) = \frac{r_{b_{num}}(\mathrm{z}) - r_{b_{int}}(\mathrm{z})}{r_{b_{num}}(\mathrm{z})} \cdot 100\%, \quad (3)$$

where $r_{b_{num}}(\mathrm{z})$ is numerical and $r_{b_{int}}(\mathrm{z})$ is interpolated values of beam radius r_b.

Generally, described above method of interpolation of electron beam boundary trajectory is based on the presumption, that dependence $r_{b_{num}}(z)$ is considered as ravine one with one global minimum and quasilinear dependence outside the region of minimum. This presumption is fully corresponded to the conception of physics of the flows of charged particles, have been described in [1–6]. Provided theoretical researches shown, that main particularities of root-polynomial function (2) are usually generally suitable to this presumption. Therefore, the interpolation error, defined by relation (3), is always very small, range of few percent, and in some cases is even smaller [47–49]. Typical dependence of obtained relative error of interpolation on z coordinate for different order of polynomial function (2) is presented in Fig. 1 [49]. In this figure the solid line corresponded to a second-order function, the dotted line – to a third-order function, the dashed line – to a fourth-order function, and the dash-dotted line – to a fifth-order function. Model parameters for the numerical data, presented at Fig. 1, are follows: $U_{ac} = 10$ kV, $I_b = 0.5$ A, $p = 0.1$ Pa.

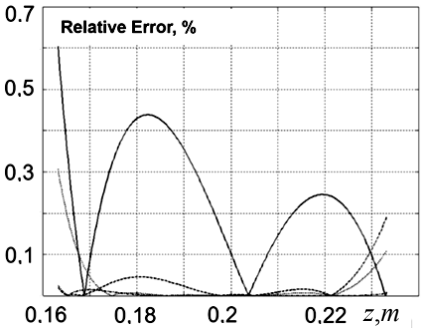

Fig. 1. Errors of interpolation of the boundary trajectory of the electron beam depend on *z* coordinate [49]

Also provided researches shown, that the interpolation error is strongly depend on position of interpolation points $P_i(r_{b_i}, z_i)$ on the interpolated interval. It has been proven, that the minimum error of interpolation is provided to symmetric interval of ravine data with location minimum in the medium point. And if the ravine data is asymmetric, the value of error is significantly increased. Namely this established rule constituted a theoretical basis for further research, which will be described later in this article.

By the reason of results of this researches the method of interpolation by higher-order root-polynomial functions is proposed, which will be considered in next section of the article.

In the paper [50] was described the method of approximation of the trajectories of electron beams, propagated in ionized gas, using third-order root-polynomial function (2). Another approach to simulation of focal beam parameters of HVGD electron guns was given in the paper [51].

ASYMMETRIC RAVINE NUMERICAL DATA AND STATEMENT THE PROBLEM OF ITS INTERPOLATION AND EXTRAPOLATION

Let's considering left-hand and right-hand asymmetric ravine root-polynomial functions, which in general form presented in Fig. 2. Here given the basic parameters of these functions, such as radiuses of electron beam in the Start Point SP r_{start} and End Point EP r_{end}, location of this points z_{start} and z_{end}, and position of beam focus z_f.

It is clear from Fig. 2, that, corresponding to the theory of interpolation, basic principles of numerical methods, and probability theory [52–58], for interpola-

tion ravine dependences using root-polynomial functions (2) the additional reference point with coordinate z_{bp} is considered, and its location is defined by following arithmetic-logic relation:

$$z_{bp}(i)=(r_{end}>r_{start})\cdot\left(\begin{pmatrix} r(i)<r_{start} \\ i_0=1; i=i+1 \end{pmatrix}\cdot z(i)+\begin{pmatrix} r(i)\geq r_{start} \\ i=i+1 \end{pmatrix}\cdot z_{bp}(i-1)\right)+$$

$$+(r_{start}\geq r_{end})\cdot\left(\begin{pmatrix} r(i)<r_{end} \\ i_0=N_P; i=i-1 \end{pmatrix}\cdot z(i)+\begin{pmatrix} r(i)\geq r_{end} \\ i=i-1 \end{pmatrix}\cdot z_{bp}(i+1)\right), \qquad (4)$$

where N_p is the whole number of points in numerical calculation of beam trajectories, which is usually in range $N_P>10^4$. On the contrary, the value of the basic points N_{BP} for solving interpolation tasks is significantly smaller: $N_{BP}=n+1$.

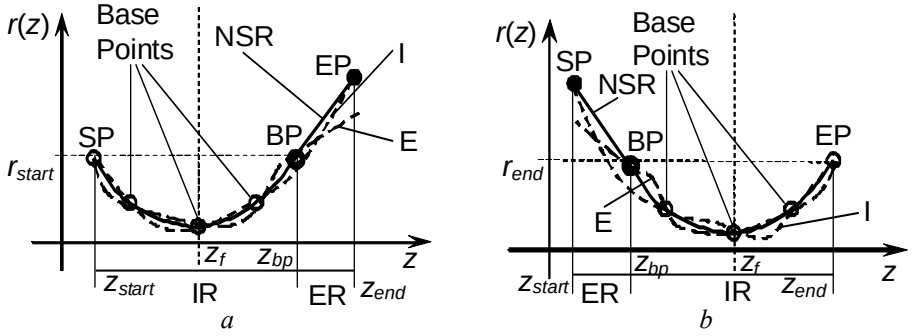

Fig. 2. Right-hand (*a*) and left-hand (*b*) asymmetric ravine functions: IR — Interpolation Region; ER — Extrapolation Region; SP — Start Point; EP — End Point; BP — Boundary Point; NSR — numerical simulation result; I — interpolation result; E — extrapolation result

The basic principles of forming arithmetic-logic relations have been considered in the book chapter [45].

After using iterative relation (4), finding of location of basic points BP on interval $[z_{start}, z_{bp}]$ for right-hand asymmetric function or in interval $[z_{bp}, z_{end}]$ for left-hand one is defined by following relations:

$$N_{BP}(j)=(z_j\geq z_f)\,N_f(1+k_f(j))+(z_j<z_f)N_f(1-k_f(j)), \qquad (5)$$

where $k_f(j)$ is the coefficient, which depend on the order of root-polynomial function and provided the minimal error of interpolation for symmetric ravine numerical data. For functions of even order usually one basis point is located at the focus position z_f and other symmetrically on the interval of interpolation $[z_{start}, z_{bp}]$ or $[z_{bp}, z_{end}]$. For example, for fifth-order root polynomial function: $k_f(2)=\frac{1}{3}$ and $k_f(3)=\frac{1}{20}$. For six-order function: $k_f(2)=\frac{1}{3}$ and $k_f(3)=\frac{1}{3}$. Correspondent approach to calculation the coefficients $k_f(j)$ is related with the theory of numerical methods [52; 53; 55; 56] and was considered in the paper [49]. Really, for symmetric ravine function:

$$\left(\left\lceil \frac{N_p}{2} \right\rceil - lk_f(l)N_p\right) = \left(\left\lceil \frac{N_p}{2} \right\rceil + lk_f(l)N_p\right), \quad l = \begin{cases} \left[1; \left\lfloor \frac{n+1}{2} \right\rfloor\right], \text{ for odd } n; \\ \left[1; \left\lfloor \frac{n}{2} \right\rfloor\right], \text{ for even } n. \end{cases} \quad (6)$$

For asymmetric ravine function problem of minimizing error of interpolation can be solved by to following ways.

1. Using interpolation method with defining position of basic points by relations (4)–(6). In this case the points are located evenly on interval $[z_{start}, z_{end}]$, and the focus position z_p can't be considered as a region of minimal error, because the coefficients k_f are calculated for ravine function.

2. Using interpolation method with defining position of basic points by relations (4)–(6) only for the symmetric region IR (see Fig. 2), and for region ER solving extrapolation task [53; 54]. In this case the additional basic boundary point BP is defined by relation (4) and used. Therefore, corresponding to Fig. 2, for right-hand asymmetric ravine data interpolation provided on the interval $[z_{start}, z_{bp}]$, and extrapolation on the interval $[z_{bp}, z_{end}]$. In contrary, for left-hand asymmetric ravine data interval of extrapolation is $[z_{start}, z_{bp}]$ and interval of interpolation is $[z_{bp}, z_{end}]$. For such self-connected interpolation-extrapolation task maximal error is always observed on the region ER, but in the region of focus position it is minimized.

Other method of interpolation, which give the average value of error on the whole interpolation interval, will be considered in the next section of the article.

INTERPOLATION OF ASYMMETRIC RAVINE NUMERICAL DATA USING ROOT-POLYNOMIAL FUNCTION OF HIGHER ORDER

The main distinguishing feature of proposed method of interpolation is solving of interpolation task on the whole interval of asymmetric ravine function $[z_{start}, z_{end}]$, but with including into consideration the boundary point BP, which coordinate, corresponding to Fig. 2, is z_{bp}. In such conditions other basic point are located in the IR region, but in ER region used interpolation by root-polynomial function (2) with the same polynomial coefficients. The order of this function is N_{BP}, where N_{BP} is number of basic points, located in the IR region. Therefore, all basic points are located evenly in interpolation interval IE using relations (4)–(6). The arithmetic-logic relation for defining set of coefficients $\{C_n \ldots C_0\}$ of the root-polynomial function of higher order $f_{n+1}(z)$ by corresponding set of basic points $\Omega(P_{start}, P_{bp}, P_{end})$ is written as follows:

$$\Omega(P_{start}, P_{bp}, P_{end}) =$$

$$= (r_{start} < r_{start}) \cdot (\{z_{start}, r_{start}\}, \{z_{BP_j}, r_{BP_j}\}\Big|_{j=1\ldots n-2}, \{z_{bp}, r_{bp}\}, \{z_{end}, r_{end}\}) +$$

$$+ (r_{start} \geq r_{end}) \cdot (\{z_{start}, r_{start}\}, \{z_{bp}, r_{bp}\}, \{z_{BP_j}, r_{BP_j}\}\Big|_{j=1\ldots n-2}, \{z_{end}, r_{end}\}), \quad (7)$$

$$\Omega(C_j\Big|_{j=0}^{j=n+1}) = \mathbf{F}(z_j\Big|_{j=0}^{j=n+1}, r_j\Big|_{j=0}^{j=n+1}).$$

Analytical relations for defining the set of coefficients of the root-polynomial function $\Omega(C_j\Big|_{j=0}^{j=n+1})$ through vector-function $\mathbf{F}(z_j\Big|_{j=0}^{j=n+1}, r_j\Big|_{j=0}^{j=n+1})$ for function from second to sixth order have been given and analyzed in the paper [49].

Some examples of using relations (4)–(7) for defining the coefficient of root-polynomial function (2), as well as comparing the error of interpolation using high-order, low-order functions and combined interpolation-extrapolation method, will be presented in the next part of the article.

OBTAINED RESULTS OF INTERPOLATION AND EXTRAPOLATION OF ASYMMETRIC RAVINE NUMERICAL DATA USING ROOT-POLYNOMIAL FUNCTION OF LOW AND HIGHER ORDER

Comparing study of applying interpolation and combined interpolation-extrapolation methods, described above, has been provided by comparing such types of errors: maximal error $\varepsilon_{\max}$, average error ε_{av}, error of estimation the focus position ε_F, and error of estimation focal beam radius ε_{rf}.

Average error is defined by the well-known method of optimization technique [53; 54] and of mathematical statistics [57; 58] as follows:

$$\varepsilon_{av} = \frac{\sum_{i=1}^{N_p} |r_{est} - r_{sim}|}{N_p}, \tag{8}$$

where r_{sim} is the radius of the electron beam, calculated numerically by the set of equations (1) using the fourth-order Runge-Kutt method [55; 56], and r_{est} is the value of the beam radius, estimated using relation (2). Local error of interpolation and extrapolation at considered point z has been defined, using relation (3).

All errors have been estimated for different order of root-polynomial functions n and length of extrapolation region L_{add}. Task parameter L_{add} is given in the tables of obtained testing results in absolute value, in meters, and relatively to the length of the interpolation region IR, in percents.

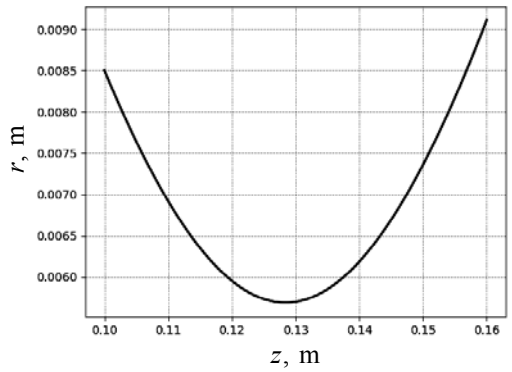

Fig. 3. Dependence $r(z)$ for $U_{ac} = 15\,\text{kV}$, $I_b = 5.5\,\text{A}$, $P = 4.5\,\text{Pa}$, end point $z_{end} = 0.16\,\text{m}$ (screen copy)

Task 1. $U_{ac} = 15\,\text{kV}$, $I_b = 5.5\,\text{A}$, $p = 4.5\,\text{Pa}$, $r_{start} = 8.5\,\text{mm}$, $\theta = 10.5^0$, $z_{start} = 0.1\,\text{m}$. End points: 1. $z_{end} = 0.16\,\text{m}$; 2. $z_{end} = 0.165\,m$; 3. $z_{end} = 0.17\,\text{m}$; 4. $z_{end} = 0.175\,\text{m}$; 5. $z_{end} = 0.18$. Additional boundary basic point: $z_{bp} = 0.156822\,\text{m}$.

For this example, the dependence $r(z)$, defined by numerical solving the set of equations (1), is presented in Fig. 3.

It is clear that the dependence presented in Fig. 3, corresponding to classification, given at Fig. 2, is a right-hand asymmetric ravine function. Errors in solving interpolation and self-connected interpolation-extrapolation tasks for this example are presented in Table 1. Corresponded polynomial coefficients are given in Table 2.

It is clear that the dependence presented in Fig. 3, corresponding to classification, given at Fig. 2, is a right-hand asymmetric ravine function. Errors in solving interpolation and self-connected interpolation-extrapolation tasks for this example are presented in Table 1. Corresponded polynomial coefficients are given in Table 2.

T a b l e 1. Errors of estimation for Task 1

Type of Error	Estimation methods								L_{addb}, m /%
	Interpolation Function Order, n			Extrapolation Function Order, n			Orders n_h of Higher-Order Method		
	4	5	6	4	5	6	5	6	
ε_{max}, %	0.51	0.865	0.118	1.355	2.26	0.76	3.2	0.26	$3.17\cdot10^{-3}$ / 5.6
ε_{av}, %	0.1586	0.377	$3\cdot10^{-2}$	0.19	0.338	$6\cdot10^{-2}$	0.926	0.11	
ε_F, %	$3.73\cdot10^{-2}$	$9.3\cdot10^{-3}$	$1.87\cdot10^{-2}$	0	0	0	0.129	0	
ε_{rf}, %	$1.45\cdot10^{-4}$	0.1536	$4.07\cdot10^{-5}$	$4.33\cdot10^{-12}$	$6.8\cdot10^{-12}$	$7.12\cdot10^{-10}$	0.014	$5\cdot10^{-2}$	
ε_{max}, %	0.98	1.434	0.281	1.355	2.26	0.76	3.35	0.3	$3.82\cdot10^{-3}$ / 14.388
ε_{av}, %	0.275	0.595	$6.6\cdot10^{-2}$	0.19	0.338	0.059	0.96	0.16	
ε_F, %	0.1367	$2\cdot10^{-2}$	$7.1\cdot10^{-2}$	0	0	0	0.82	0	
ε_{rf}, %	$2\cdot10^{-3}$	0.25	$5.3\cdot10^{-4}$	$4.33\cdot10^{-12}$	0.068	$7.12\cdot10^{-10}$	0.069	0.0533	
ε_{max}, %	1.615	2.263	0.537	2.65	4.45	1.72	4.616	0.843	$1.3175\cdot10^{-2}$ / 23.187
ε_{av}, %	0.47	0.9	0.1376	0.323	0.55	0.147	1.4	0.31	
ε_F, %	0.294	$6\cdot10^{-2}$	0.17445	0	0	0	0.36	0	
ε_{rf}, %	$8.8\cdot10^{-3}$	0.394	$3.4\cdot10^{-3}$	$1.32\cdot10^{-11}$	0.0544	$1.25\cdot10^{-9}$	0.0136	0.2478	
ε_{max}, %	2.4	3.447	0.89	4.13	6.92	2.9	2.7845	0.563	$1.8175\cdot10^{-2}$ / 32
ε_{av}, %	0.7465	1.33	0.256	0.53	0.9	0.2925	0.908	0.24	
ε_F, %	0.5257	0.1577	0.345	$5.84\cdot10^{-3}$	0	0	1.0	0	
ε_{rf}, %	$2.8\cdot10^{-2}$	0.6	$1.39\cdot10^{-2}$	$3.89\cdot10^{-7}$	0.0454	$3\cdot10^{-11}$	0.1147	0.0563	
ε_{max}, %	1.219	5.11	1.32	5.8	9.6	4.367	3.13	0.977	$2.1375\cdot10^{-2}$ / 40.8
ε_{av}, %	3.385	1.87	0.432	0.8166	1.379	0.51725	1.1168	0.37	
ε_F, %	3.078	0.6541	0.6168	0	0	0	1.05	0	
ε_{rf}, %	1.4	0.8752	$4.67\cdot10^{-2}$	$9.76\cdot10^{-12}$	0.0389	$4.28\cdot10^{-12}$	0.13	0.06	

T a b l e 2. Coefficients of root-polynomial function (2) for Task 1, z_{end} = 0.16 m

Estimation methods	n	Coefficients of root-polynomial function (2)						
		C_6	C_5	C_4	C_3	C_2	C_1	C_0
Lower-order interpolation	4	–	–	$3.14\cdot10^{3}$	$-1.6\cdot10^{3}$	$3.13\cdot10^{4}$	$-2.72\cdot10^{5}$	$8.96\cdot10^{7}$
	5	–	$4.944\cdot10^{-5}$	$9.97\cdot10^{6}$	$-1.33\cdot10^{5}$	$3.1\cdot10^{6}$	$-2.6\cdot10^{7}$	$9.9\cdot10^{9}$
	6	$2.2\cdot10^{4}$	$-1.7\cdot10^{-4}$	$5.487\cdot10^{-5}$	$9.45\cdot10^{6}$	$9.184\cdot10^{-7}$	$-4.778\cdot10^{8}$	$1.04\cdot10^{9}$
Interpolation and extrapolation	4	–	–	$3.06\cdot10^{3}$	$-1.57\cdot10^{3}$	$3.05\cdot10^{4}$	$-2.66\cdot10^{5}$	$8.774\cdot10^{7}$
	5	–	$-8.96\cdot10^{7}$	$3.98\cdot10^{5}$	$-2.03\cdot10^{5}$	$3.9\cdot10^{6}$	$-3.37\cdot10^{7}$	$1.1\cdot10^{8}$
	6	$2.11\cdot10^{4}$	$-1.626\cdot10^{-4}$	$5.239\cdot10^{-5}$	$-9.036\cdot10^{6}$	$8.798\cdot10^{-7}$	$-4.586\cdot10^{8}$	10^{9}
Higher-order interpolation	5	–	$4.84\cdot10^{-4}$	$2.744\cdot10^{-4}$	$6.074\cdot10^{-5}$	$-6.474\cdot10^{-6}$	$-3.245\cdot10^{-7}$	$-5.8\cdot10^{9}$
	6	$2.63\cdot10^{4}$	$-2.03\cdot10^{4}$	$6.53\cdot10^{5}$	$-1.222\cdot10^{-5}$	$1.1\cdot10^{-6}$	$-5.63\cdot10^{8}$	$1.22\cdot10^{9}$

Results of estimations in graphic form for the point $z_{end} = 0.16$ m are presented at Fig. 4.

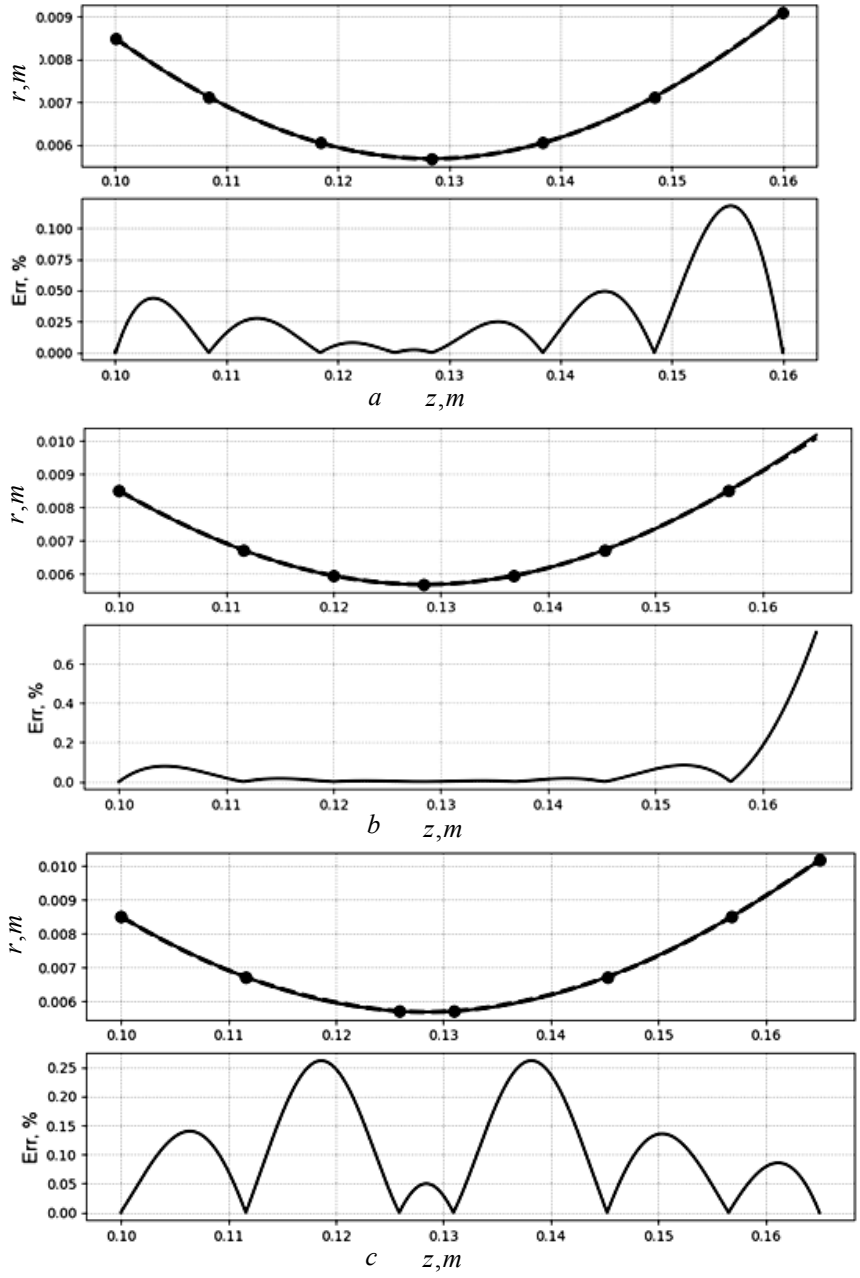

Fig. 4. Lower-order interpolation (*a*), extrapolation (*b*) and higher-order interpolation (*c*) for the Task 1, $n = 6$

In the upper graphs straight line correspond to numerical solving the set of equation (1) and dash line to estimation of numerical solution in dependences on length of propagation of electron beam. On the lower graphs shown the error of estimation in dependences on length of propagation of electron beam (screen copy).

Dependence of error of estimation for extrapolation and higher-order interpolation tasks on the length of extrapolation region L_{add} for different orders of root-polynomial function presented at Fig. 5.

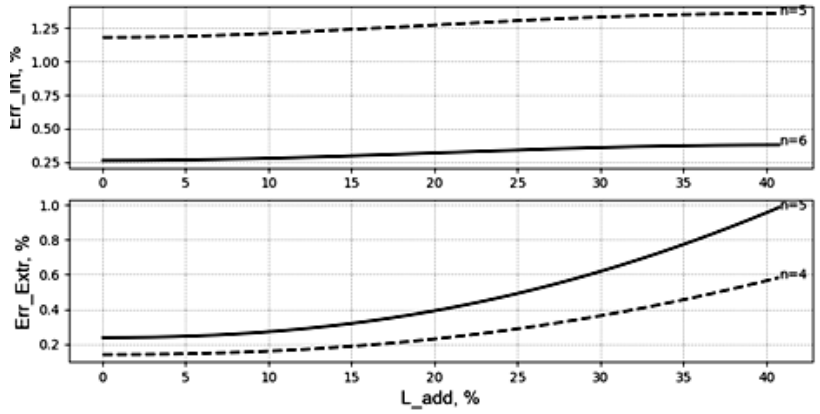

Fig. 5. Dependences of errors of higher-order interpolation (upper) and extrapolation (lower) tasks on the relative length of extrapolation region L_{add} and order of root-polynomial function n for Task 1 (screen copy)

Task 2. $U_{ac} = 15\,\text{kV}$; $I_b = 5.5\,\text{A}$, $p = 4.5\,\text{Pa}$, $r_{srart} = 8.5\,\text{mm}$, $\theta = 10.5^0$, $z_{start} = 0.1\,\text{m}$. End points: $z_{end} = 0.155\,\text{m}$, $z_{end} = 0.153\,\text{m}$, $z_{end} = 0.15\,\text{m}$, $z_{end} = 0.147\,\text{m}$, and $z_{end} = 0.145\,\text{m}$.

For this example, the dependence $r(z)$, defined by numerical solving the set of equations (1), is presented in Fig 6.

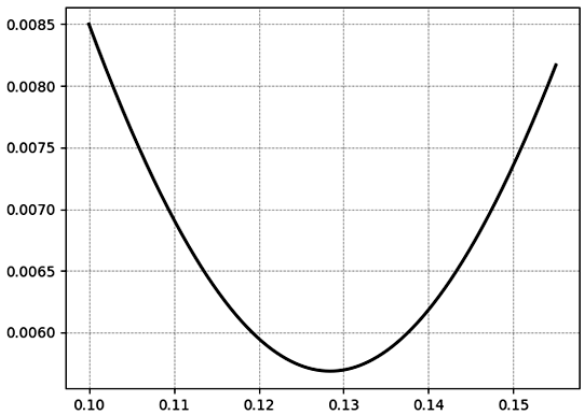

Fig. 6. Dependence $r(z)$ for $U_{ac} = 15\,\text{kV}$, $I_b = 5.5\,\text{A}$, $P = 4{,}5\,\text{Pa}$, end point $z_{end} = 0.155\,\text{m}$ (screen copy)

It is clear that the dependence presented in Fig. 6, corresponding to classification, given at Fig. 2, is a left-hand asymmetric ravine function. The position of boundary point for left-hand asymmetric are always different. Corresponded values for this task are presented at Table 3. Errors in solving interpolation and self-connected interpolation-extrapolation tasks for this example are presented in Table 4. Obtained polynomial coefficients for different estimation methods are given in Table 5.

Table 3. Position of boundary points z_{bp} in depend on position of end point z_{end} for left-hand asymmetric ravine function, given in Task 2

z_{end}, m	0.155	0.153	0.15	0.147	0.145
z_{bp}, m	0.102	0.1038	0.1044	0.1074	0.10942

Table 4. Errors of estimation for Task 2

Type of Error	Estimation methods								L_{add}, m / %
	Interpolation Function Order, n			Extrapolation Function Order, n			Orders n_h of Higher-Order Method		
	4	5	6	4	5	6	5	6	
ε_{max}, %	0.344	0.5224	$6.6\cdot10^{-2}$	0.2357	0.38	0.0735	1.347	0.145	$1.83\cdot10^{-3}$ / 3.44
ε_{av}, %	0.1	0.24	$1.7\cdot10^{-2}$	$9.147\cdot10^{-2}$	0.1887	0.01455	0.4	$5.65\cdot10^{-2}$	
ε_F, %	$3\cdot10^{-2}$	$4.3\cdot10^{-3}$	$4.3\cdot10^{-3}$	0	0	0	0.6425	0	
ε_{rf}, %	$8.62\cdot10^{5}$	0.09	$3.89\cdot10^{-6}$	$1.24\cdot10^{-11}$	0.0634	$1.91\cdot10^{-9}$	$4.426\cdot10^{-2}$	0.0297	
ε_{max}, %	0.344	0.44	$7.54\cdot10^{-2}$	0.38143	0.63	0.164	1.03	0.084	$3.8\cdot10^{-3}$ / 7.79
ε_{av}, %	$9.7\cdot10^{-2}$	0.202	$1.58\cdot10^{-2}$	0.0736	0.134	0.0137	0.3	0.0343	
ε_F, %	$3\cdot10^{-2}$	$4.1\cdot10^{-3}$	$8.26\cdot10^{-3}$	0	0	0	0.425	0	
ε_{rf}, %	$8.62\cdot10^{-2}$	$7.07\cdot10^{-2}$	$1.05\cdot10^{-5}$	$1.34\cdot10^{-11}$	0.0336	$1.14\cdot10^{-9}$	$1.94\cdot10^{-2}$	$1.5\cdot10^{-2}$	
ε_{max}, %	0.3725	0.3685	$8.97\cdot10^{-2}$	0.66	1.17	0.3	0.6386	0.034	$4.415\cdot10^{-3}$ / 9.685
ε_{av}, %	0.096	0.1628	$1.69\cdot10^{-2}$	0.069	0.12	0.019	0.172	0.0185	
ε_F, %	$4.3\cdot10^{-2}$	$3.893\cdot10^{-3}$	$1.16\cdot10^{-2}$	0	0	0	0.214	0	
ε_{rf}, %	$1.79\cdot10^{-4}$	$4.87\cdot10^{-2}$	$1.3\cdot10^{-2}$	$1.3\cdot10^{-11}$	0.012	$3.44\cdot10^{-10}$	$5\cdot10^{-3}$	$5.4\cdot10^{-3}$	
ε_{max}, %	0.3224	0.5224	$6.6\cdot10^{-2}$	0.2357	0.38	$7.35\cdot10^{-2}$	1.347	0.145	$7.422\cdot10^{-3}$ / 18.75
ε_{av}, %	0.1054	0.24	$1.7\cdot10^{-2}$	$9.15\cdot10^{-2}$	0.1887	$1.45\cdot10^{-2}$	0.4	$5.65\cdot10^{-2}$	
ε_F, %	0.017	$4.3\cdot10^{-3}$	$4.3\cdot10^{-3}$	0	0	0	0.6425	0	
ε_{rf}, %	$2.52\cdot10^{-5}$	$8.9\cdot10^{-2}$	$3.89\cdot10^{-2}$	$1.24\cdot10^{-11}$	$6.34\cdot10^{-2}$	$1.91\cdot10^{-9}$	$4.4\cdot10^{-2}$	$2.97\cdot10^{-2}$	
ε_{max}, %	0.4	0.398	0.112361	1.107	2.073	0.58	0.22	$7.66\cdot10^{-2}$	$9.42\cdot10^{-2}$ / 26.5
ε_{av}, %	0.11	0.129	$2.2\cdot10^{-2}$	0.11	0.2065	$4.81\cdot10^{-2}$	0.084	$1.66\cdot10^{-2}$	
ε_F, %	0.042	$3.5\cdot10^{-3}$	$1.05\cdot10^{-2}$	0	0	0	0.06	0	
ε_{rf}, %	$1.95\cdot10^{-4}$	0.024	$1.31\cdot10^{-5}$	$9.1\cdot10^{-12}$	$1.54\cdot10^{-3}$	$9.76\cdot10^{-10}$	$4.08\cdot10^{-4}$	$7.3\cdot10^{-4}$	

Table 5. Coefficients of root-polynomial function (2) for Task 2, $z_{end} = 0.15$ m

Estimation methods	n	Coefficients of root-polynomial function (2)						
		C_6	C_5	C_4	C_3	C_2	C_1	C_0
Lower-order interpolation	4	–	–	$2.95\cdot10^{3}$	$-1.512\cdot10^{-3}$	$2.956\cdot10^{-4}$	$-2.582\cdot10^{-5}$	$8.538\cdot10^{-7}$
	5	–	$-9.963\cdot10^{-5}$	$9.966\cdot10^{-5}$	$-3.4734\cdot10^{-5}$	$5.6475\cdot10^{-6}$	$-4.408\cdot10^{-7}$	$1.34\cdot10^{-8}$
	6	$2\cdot10^{-4}$	$-1.549\cdot10^{-4}$	$5\cdot10^{-5}$	$-8.64\cdot10^{-6}$	$8.43\cdot10^{-7}$	$-4.4046\cdot10^{-8}$	$9.628\cdot10^{-10}$
Interpolation and extrapolation	4	–	–	$2.8\cdot10^{-3}$	$-1.435\cdot10^{-3}$	$2.792\cdot10^{-4}$	$-2.43\cdot10^{-5}$	$8.06\cdot10^{-7}$
	5	–	$-8.5335\cdot10^{-7}$	$3.25\cdot10^{-5}$	$-1.655\cdot10^{-5}$	$3.198\cdot10^{-6}$	$-2.766\cdot10^{-7}$	$9.032\cdot10^{-9}$
	6	$1.84\cdot10^{-4}$	$-1.417\cdot10^{-4}$	$4.57\cdot10^{-5}$	$-7.9\cdot10^{-6}$	$7.7\cdot10^{-7}$	$-4.03\cdot10^{-8}$	$8.821\cdot10^{-10}$
Higher-order interpolation	5	–	$4.03\cdot10^{-4}$	$2.9\cdot10^{-4}$	$-8.2\cdot10^{-5}$	$1.15\cdot10^{-5}$	$-8.018\cdot10^{-7}$	$2.227\cdot10^{-8}$
	6	$2.22\cdot10^{-4}$	$-1.71\cdot10^{-4}$	$5.51\cdot10^{-5}$	$-9.495\cdot10^{-6}$	$9.235\cdot10^{-7}$	$-4.81\cdot10^{-8}$	$1.046\cdot10^{-9}$

Results of estimations in graphic form for the point $z_{end} = 0.15$ m are presented at Fig. 7. Dependence of error of estimation for extrapolation and higher-order interpolation tasks on the length of extrapolation region L_{add} for different orders of root-polynomial function presented at Fig. 8.

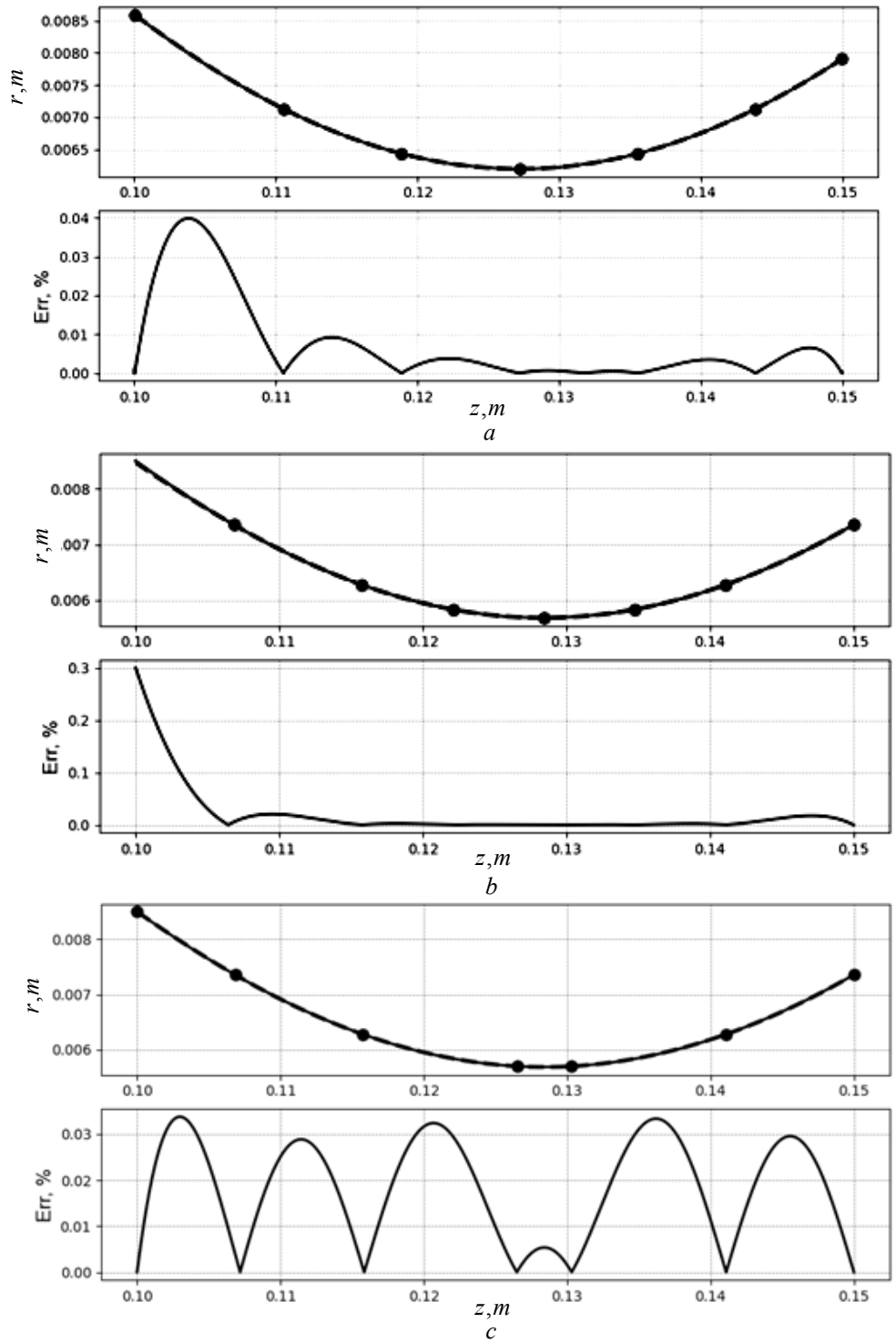

Fig. 7. Lower-order interpolation (*a*), extrapolation (*b*) and higher-order interpolation (*c*) for the Task 2, $n = 6$. In the upper graphs straight line correspond to numerical solving the set of equation (1) and dash line to estimation of numerical solution in dependences on length of propagation of electron beam. On the lower graphs shown the error of estimation in dependences on length of propagation of electron beam (screen copy)

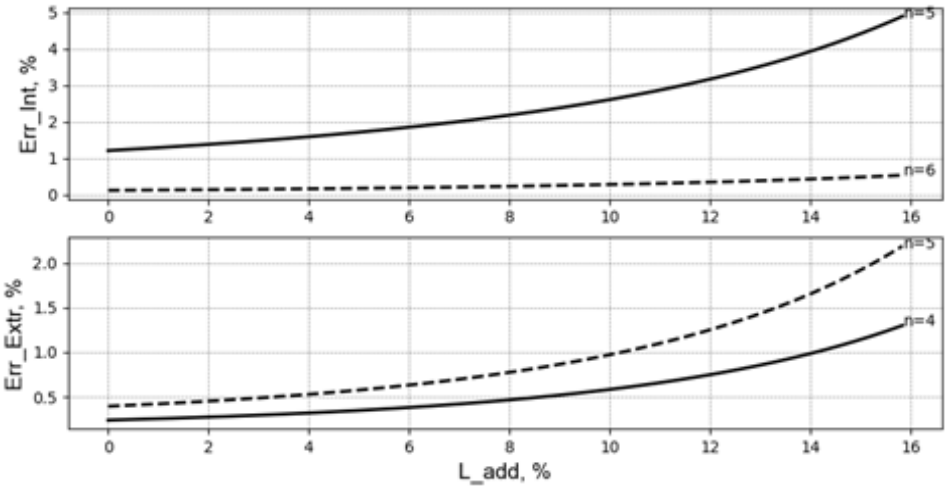

Fig. 8. Dependences of errors of higher-order interpolation (upper) and extrapolation (lower) tasks on the relative length of extrapolation region L_{add} and order of root-polynomial function n for Task 1 (screen copy)

PARTICULARITIES OF ELABORATED COMPUTER SOFTWARE

All simulation results presented in this paper have been obtained using original software, which has been elaborated for simulation and numerical estimation of the boundary trajectory of an electron beam propagated in ionized gas. The source program code has been written using the means of programing language Python, including advanced mathematic and graphic libraries such as tkinter, nympy, and matplotlib [59; 60]. The distinguishing feature of elaborated software from the point of view of the means of programming is including additional advanced libraries for creating scientific plots from module matplotlib into traditional elements of the interface window created using the function of module tkinter [59; 60]. For the correct solution of this sophisticated programming task, specific system tools have been used, including the definition of virtual variables and creating on its base the virtual environment for forming a virtual disk in the operative memory of a local computer [59; 60]. Corresponding graphic interface windows of elaborated software for the bookmarks "Interpolation" and "Extrapolation" are presented in Fig. 9. For saving and further analyzing the obtained graphic information, the bottom "Save Graph" has been provided in both interface windows.

For automatic creation of root-polynomial functions on both bookmarks, the bottoms "Import from SDE Task" have been provided. Using this program's functionality is possible only after solving the simulation task for the established electron beam parameters in the corresponded bookmark "Solving of Differential Equation of Beam Boundary Trajectory". But the manual creation of the root-polynomial function by the r and z coordinates, which have to be input in the corresponded textboxes, is also possible by pressing the bottom "Calculate Manually".

Errors of estimation, presented in Tables 1 and 4, as well as coefficients of root-polynomial functions, presented in Tables 2 and 5, are written out in the established output text windows on the corresponded bookmarks. All described elements of the graphic user interface are shown in the copy of these bookmarks, presented in Fig. 9.

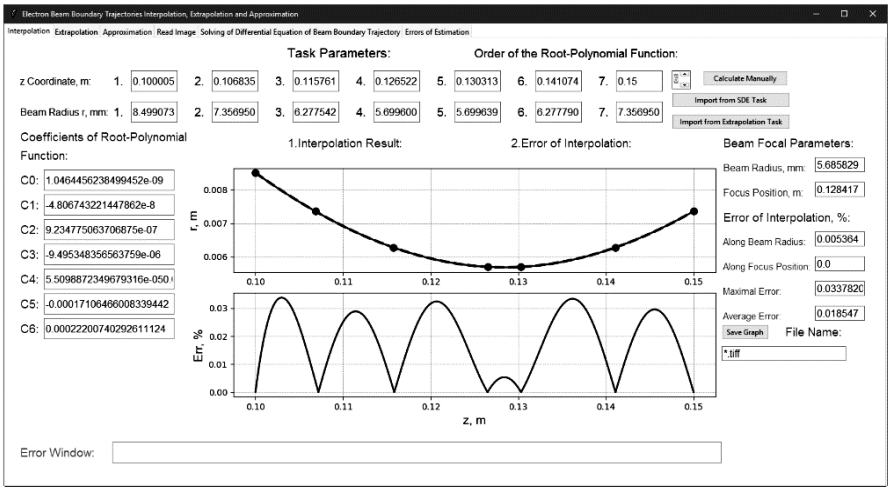

a

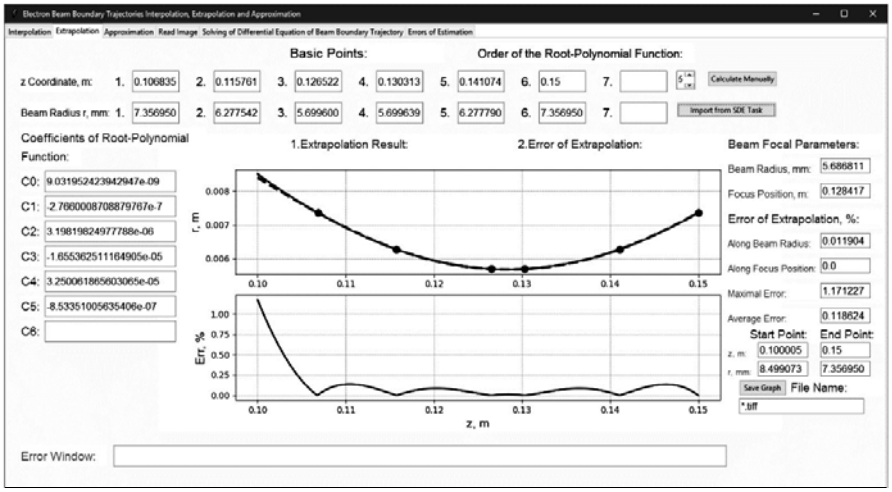

b

Fig. 9. Interface windows for bookmarking “Interpolation” (*a*) and “Extrapolation” (*b*) in elaborated computer software (screen copy)

ANALYSIS OF OBTINED RESULTS AND DISCUSSION

The computer simulation results described in this paper showed that higher-order interpolation for asymmetric ravine functions gives an average error value. No minimum error value was detected for this novel estimation method. In general, from a theoretical point of view, this is due to the location of the reference points for root-polynomial functions of the appropriate order. Indeed, the k_f values determined by relations (5), (6) were chosen correctly only for the corresponded lower-order of the odd or even root polynomial function (2).

For example, for higher-order interpolation with order of function $n_h = 5$, the basic points are located as for forth order symmetric function, and additional point, located at the start of interpolated interval for left-hand asymmetric function or on the end of this interval for right-hand asymmetric function, is artificially added.

Generally, corresponding to Tables 1 and 4, minimal values of maximal and average interpolation error are corresponded to standard low-order interpolation,

but self-connected interpolation-extrapolation task usually given the minimal errors in estimation of focal parameters of electron beam. The same conclusion are follows from graphic dependences, presented at Fig. 4 and Fig. 7.

But, in any case, average integral error of estimation the beam trajectory by the higher-order root-polynomial function in the whole segment of interpolation isn't so large, therefore such estimation can be preferable in some solutions for practice application. For simplifying the further corresponded analysis in the digital presentation all estimation errors for the end point $z_{end} = 0.15$ are rewritten from extended Table 4 to smaller Table 6.

Table 6. Errors of estimation for Task 2 for end point $z_{end} = 0.15$ m

Methods and function order		**Standard Interpolation**			**Interpolation and Extrapolation**			**Higher-Order Interpolation**	
N		4	5	6	4	5	6	5	6
Errors	ε_{max}, %	0.3725	0.3685	$897 \cdot 10^{-2}$	0.66	1.17	0.3	0.6386	0.034
	ε_{av}, %	0.096	0.1628	$1.69 \cdot 10^{-2}$	0.069	0.12	0.019	0.172	0.0185
	ε_F, %	$4.3 \cdot 10^{-2}$	$3.893 \cdot 10^{-3}$	1.1610^{-2}	0	0	0	0.214	0
	ε_{rf}, %	$1.79 \cdot 10^{-4}$	$4.87 \cdot 10^{-2}$	$1.3 \cdot 10^{-5}$	$1.3 \cdot 10^{-11}$	0.012	$3.44 \cdot 10^{-10}$	$5 \cdot 10^{-3}$	$5.4 \cdot 10^{-3}$

From the calculation results, presented in Table 6, it is clear, that for higher-order interpolation the for $n = 6$ average error ($\varepsilon_{av} = 0.0185$ %) isn't so small, than for standard interpolation by the function of same order ($\varepsilon_{av} = 0.0169$ %), but the difference of these errors isn't so large. Also, and it is very significant and important that the estimation using higher-order interpolation for $n = 6$ gives the minimal value of the maximal error, $\varepsilon_{max} = 0.034$ %.

It is clear also from numerical data, presented in Table 6, that the best results for estimation of focal radius of electron beam giving the method of interpolation and extrapolation by forth and six order functions, the level of error ε_{rf} is range of from 10^{-11} % to 10^{-10} %. But such precision estimation of focal beam parameters usually isn't necessary for the practical applications. Estimation using higher-order interpolation method give the value of error $\varepsilon_{rf} = 5.4 \cdot 10^{-3}$ %, which, certainly, isn't so small, but usually is suitable for the most of practical applications [16]. It is also interesting and important, that for self-connected interpolation and extrapolation method the error of estimation focus position is $\varepsilon_F = 0$ %, but the same result is observed for higher-order interpolation function in the case of $n = 6$.

As it is clear from Tables 1 and 4, the particularities of the different methods of interpolation and extrapolation described above are similar for all positions of the end point, including left-hand and right-hand ravine functions. But, in any case, the error in the estimation of electron beam boundary trajectories by using the root-polynomial function (2) is very small, in the range of a fraction of a percent. This result is confirming the pervious preliminary theoretical estimations, have been provided in the works [47–49].

All research work described in this paper has been provided in the Scientific and Educational Laboratory of Electron Beam Technological Devices of the National Technical University of Ukraine "Igor Sikorsky Kyiv Polytechnical Institute".

CONCLUSION

Generally, provided research has shown that usually the minimal average error ε_{av} of estimation of the boundary electron beam trajectory using the root-polynomial

function (2) corresponds to the lower-order interpolation method. The best orders of these functions are even values, such as $n = 2$, $n = 4$, and $n = 6$. The best estimations of electron beam focal parameters have been obtained using the self-connected interpolation-extrapolation method. The level of error in the estimation of the focal beam radius ε_{rf} for this method has been significantly small, ranging from 10^{-11} % to 10^{-10} %, and the estimation by the focus position has been exactly precise without error. The best results for this method also give the even values of the order of the root-polynomial function, such as $n = 4$ and $n = 6$. It can be generally explained by the suitable choice of base points position for the symmetric part of the ravine function, which is evaluated. The proposed method of higher-order root-polynomial interpolation gives an average value of error both in the focal region and at the start and end basic points. The larger values of the average error in this case are explained by the location of the basic points. Unfortunately, solving the optimization task of defining the basic points position in this case is impossible.

All simulation results presented in this paper have been obtained using original computer software elaborated and developed by applying the advanced mathematical and graphic means of the Python programming language.

Obtained scientific results and practical recommendations can be interesting to a wide range of experts in the fields of the physics of electron beams and advanced electron beam technologies, as well as in the computational mathematics and methods of interpolation and extrapolation of ravine functions.

REFERENCES

1. M. Reiser, *Theory and Design of Charged Particle Beams*. John Wiley & Sons, 2008, 634 p. Available: https://www.wiley.com/en-us/Theory+and+ Design +of+Charged+ Particle+Beams-p-9783527617630
2. M. Szilagyi, *Electron and Ion Optics*. Springer Science & Business Media, 2012, 539 p. Available: https://www.amazon.com/Electron-Optics-Microdevices-Miklos-Szilagyi/dp/1461282470
3. S.J.R. Humphries, *Charged Particle Beams*. Courier Corporation, 2013, 834 p. Available: https://library.uoh.edu.iq/admin/ebooks/76728-charged-particle-beams---s.-humphries.pdf
4. R.C. Davidson, H. Qin, *Physics of Intense Charged Particle Beams in High Energy Accelerators*. World Scientific, Singapore, 2001, 604 p. Available: https://books.google.com.ua/books/about/Physics_Of_Intense_Charged_Particle_Beam.html?id=5M02DwAAQBAJ&redir_esc=y
5. G. Brewer, *Electron-Beam Technology in Microelectronic Fabrication*. Elsevier, 2012, 376 p. Available: https://books.google.com.ua/books?id= snU5sOQD6noC&hl=uk&source=gbs_similarbooks
6. J.D. Lawson, *The Physics of Charged-Particle Beams*. Oxford: Clarendon Press, 1977, 446 p. Available: https://www.semanticscholar.org/paper/The-Physics-of-Charged-Particle-Beams-Stringer/80b5ee5289d5efd8f480b516ec4bade0aa529ea6
7. S. Schiller, U. Heisig, and S. Panzer, *Electron Beam Technology*. John Wiley & Sons Inc, 1995, 508 p. Available: https://books.google.com.ua/books/about/ Electron_ Beam_Technology.html?id=QRJTAAAAMAAJ&redir_esc=y
8. H. Schultz, *Electron Beam Welding*. Woodhead Publishing, 1993, 240 p. Available: https://books.google.com.ua/books?id=I0xMo28DwcIC&hl=uk&source= gbs_book_similarbooks
9. R.A. Bakish, *Introduction to Electron Beam Technology*. Wiley, 1962, 452 p. Available: https://books.google.com.ua/books?id=GghTAAAAMAAJ&hl= uk&source= gbs_similarbooks

10. T. Kemmotsu, T. Nagai, and M. Maeda, "Removal Rate of Phosphorous form Melting Silicon," *High Temperature Materials and Processes*, vol. 30, issue 1–2, pp. 17–22, 2011. Available: https://www.degruyter.com/journal/key/ htmp/30/1-2/html
11. J.C.S. Pires, A.F.B. Barga, and P.R. May, "The purification of metallurgically grade silicon by electron beam melting," *Journal of Materials Processing Technology*, vol. 169, no. 1, pp. 347–355, 2005. Available: https://www.academia.edu/9442020/ The_purification_of_metallurgical_grade_silicon_by_electron_beam_melting
12. D. Luo, N. Liu, Y. Lu, G.Zhang, and T. Li, "Removal of impurities from metallurgically grade silicon by electron beam melting," *Journal of Semiconductors*, vol. 32, issue 3, article ID 033003, 2011. Available: http://www.jos.ac.cn/en/article/ doi/10.1088/1674-4926/32/3/033003
13. D. Jiang, Y. Tan, S. Shi, W. Dong, Z. Gu, and R. Zou, "Removal of phosphorous in molten silicon by electron beam candle melting," *Materials Letters*, vol. 78, pp. 4–7, 2012.
14. A.A. Druzhinin, I.P. Ostrovskii, Y.N. Khoverko, N.S.Liakh-Kaguy, and A.M. Vuytsyk, "Low temperature characteristics of germanium whiskers," *Functional materials 21*, no. 2, pp. 130–136, 2014. Available: http://dspace.nbuv.gov.ua/bitstream/ handle/123456789/120404/02-Druzhinin.pdf?sequence=1
15. A.A. Druzhinin, I.A. Bolshakova, I.P. Ostrovskii, Y.N. Khoverko, and N.S. Liakh-Kaguy, "Low temperature magnetoresistance of InSb whiskers," *Materials Science in Semiconductor Processing*, vol. 40, pp. 550–555, 2015. Available: https://academic-accelerator.com/search?Journal=Druzhinin
16. I. Melnyk, S. Tuhai, M. Surzhykov, I. Shved, V. Melnyk, and D. Kovalchuk, "Analytical Estimation of the Deep of Seam Penetration for the Electron-Beam Welding Technologies with Application of Glow Discharge Electron Guns," *2022 IEEE 41-st International Conference on Electronics and Nanotechnology (ELNANO), 2022*, pp. 1–5. doi: 10.1109/ELNANO54667_2022_9927071
17. I. Melnyk, S. Tuhai, and A. Pochynok, "Calculation of Focal Paramters of Electron Beam Formed in Soft Vacuum at the Plane which Sloped to Beam Axis," *The Forth IEEE International Conference on Information-Communication Technologies and Radioelectronics UkrMiCo'2019. Collections of Proceedings of the Scientific and Technical Conference, Odesa, Ukraine, September 9-13, 2019*. doi: 10.1109/UkrMiCo47782.2019.9165328
18. A. Zakharov, S. Rozenko, S. Litvintsev, and M. Ilchenko, "Trisection Bandpass Filter with Mixed Cross-Coupling and Different Paths for Signal Propagation," *IEEE Microwave Wireless Component Letters*, vol. 30, no. 1, pp. 12–15, Jan. 2020. doi: 10.1109/LMWC.2019.2957207
19. A. Zakharov, S. Litvintsev, and M. Ilchenko, "Trisection Bandpass Filters with All Mixed Couplings," *IEEE Microwave Wireless Components Letter*, vol. 29, no. 9, pp. 592–594, 2019. Available: https://ieeexplore.ieee.org/abstract/document/ 8782802
20. A. Zakharov, S. Rozenko, and M. Ilchenko, "Varactor-tuned microstrip bandpass filter with loop hairpin and combline resonators," *IEEE Transactions on Circuits Systems. II. Experimental Briefs*, vol. 66, no. 6, pp. 953–957, 2019. Available: https://ieeexplore.ieee.org/document/8477112
21. A. Mitchell, T. Wang, "Electron beam melting technology review," *Proceedings of the Conference "Electron Beam Melting and Refining State of the Art 2000, Reno, NV, USA, 2000*, ed. R. Bakish, pp. 2–13.
22. D.V. Kovalchuk, N.P. Kondraty, "Electron-beam remelting of titanium – problems and development prospects," *Titan 2009*, no. 1(23), pp. 29–38.
23. V.A. Savenko, N.I. Grechanyuk, and O.V. Churakov, "Electron beam refining in production of platinum and platinum-base alloys. Information 1. Electron beam refining of platinum," *Advances in Electrometallurgy*, no. 1, pp. 14–16, 2008.
24. J. Zhang et al., "Fine equiaxed β grains and superior tensile property in Ti–6Al–4V alloy deposited by coaxial electron beam wire feeding additive manufacturing," *Acta Metallurgica Sinica (English Letters)*, 33(10), pp. 1311–1320, 2020. doi: 10.1007/s40195-020-01073-5
25. D. Kovalchuk, O. Ivasishin, "Profile electron beam 3D metal printing," in *Additive Manufacturing for the Aerospace Industry*. Elsevier Inc., 2019, pp. 213–233.
26. M. Wang et al., "Microstructure and mechanical properties of Ti-6Al-4V cruciform structure fabricated by coaxial electron beam wire-feed additive manufacturing," *Journal of Alloys and Compounds*, vol. 960. article 170943. doi: https://doi.org/10.1016/ j.jallcom.2023.170943

27. T.O. Prikhna et al., "Electron-Beam and Plasma Oxidation-Resistant and Thermal-Barrier Coatings Deposited on Turbine Blades Using Cast and Powder Ni(Co)CrALY(Si) Alloys I. Fundamentals of the Production Technology, Structure, and Phase Composition of Cast NiCrAlY Alloys," *Powder Metallurgy and Metal Ceramics*, vol. 61, issue 1-2, pp. 70–76, 2022. doi: 10.1007/s11106-022-00320-x
28. T.O. Prikhna et al., "Electron-Beam and Plasma Oxidation-Resistant and Thermal-Barrier Coatings Deposited on Turbine Blades Using Cast and Powder Ni(Co)CrAlY(Si) Alloys Produced by Electron-Beam Melting II. Structure and Chemical and Phase Composition of Cast CoCrAlY Alloys," *Powder Metallurgy and Metal Ceramicsthis*, vol. 61, issue 3-4, pp. 230–237, 2022. doi: 10.1007/s11106-023-00333-0
29. I.M. Grechanyuk et al., "Electron-Beam and Plasma Oxidation-Resistant and Thermal-Barrier Coatings Deposited on Turbine Blades Using Cast and Powder Ni(Co)CrAlY(Si) Alloys Produced by Electron Beam Melting IV. Chemical and Phase Composition and Structure of Cocralysi Powder Alloys and Their Use," *Powder Metallurgy and Metal Ceramics*, vol. 61, issue 7-8, pp. 459–464, 2022. doi: 10.1007/s11106-022-00310-z
30. M.I. Grechanyuk et al., "Electron-Beam and Plasma Oxidation-Resistant and Thermal-Barrier Coatings Deposited on Turbine Blades Using Cast and Powder Ni (Co)CrAlY (Si) Alloys Produced by Electron Beam Melting III. Formation, Structure, and Chemical and Phase Composition of Thermal-Barrier Ni(Co)CrAlY/ZrO_2–Y_2O_3 Coatings Produced by Physical Vapor Deposition in One Process Cycle," *Powder Metallurgy and Metal Ceramics*, vol. 61, issue 5-6, pp. 328–336, 2022. doi: 10.1007/s11106-022-00320-x
31. A.F. Tseluyko, V.T. Lazurik, D.L. Ryabchikov, V.I. Maslov, and I.N. Sereda, "Experimental study of radiation in the wavelength range 12.2-15.8 nm from a pulsed high-current plasma diode," *Plasma Physics Reports*, 34(11), pp. 963–968, 2008. doi: 10.1134/S1063780X0811010X
32. V.G. Rudychev, V.T. Lazurik, and Y.V. Rudychev, "Influence of the electron beams incidence angles on the depth-dose distribution of the irradiated object," *Radiation Physics and Chemistry*, 186, 109527, 2021. doi: 10.1016/j.radphyschem.2021.109527
33. V.M. Lazurik, V.T. Lazurik, G. Popov, and Z. Zimek, "Two-parametric model of electron beam in computational dosimetry for radiation processing, *Radiation Physics and Chemistry*, 124, pp. 230–234, 2016. doi: 10.1016/j.radphyschem. 2015.12.00
34. I. Melnyk, S. Tuhai, and A. Pochynok, "Universal Complex Model for Estimation the Beam Current Density of High Voltage Glow Discharge Electron Guns," *Lecture Notes in Networks and Systems*; Eds: M. Ilchenko, L. Uryvsky, L. Globa, vol. 152, pp. 319–341, 2021. doi: 10.1007/978-3-030-58359-0_18
35. I.V. Melnyk, "Numerical simulation of distribution of electric field and particle trajectories in electron sources based on high-voltage glow discharge," *Radioelectronic and Communication Systems*, vol. 48, no. 6, pp. 61–71, 2005. doi: https://doi.org/10.3103/S0735272705060087
36. S.V. Denbnovetsky, J. Felba, V.I. Melnik, and I.V. Melnik, "Model of Beam Formation in a Glow Discharge Electron Gun with a Cold Cathode," *Applied Surface Science*, 111, pp. 288–294, 1997. doi: 10.1016/S0169-4332(96)00761-1
37. S.V. Denbnovetsky, V.G. Melnyk, and I.V. Melnyk, "High voltage glow discharge electron sources and possibilities of its application in industry for realizing different technological operations," *IEEE Transactions on Plasma Science*, vol. 31, issue 5, pp. 987–993, October, 2003. doi: 10.1109/TPS.2003.818444
38. S. Denbnovetskiy et al., "Principles of operation of high voltage glow discharge electron guns and particularities of its technological application," *Proceedings of SPIE, The International Society of Optical Engineering*, pp. 10445–10455, 2017. doi: 10.1117/12.2280736
39. S.V. Denbnovetsky, V.I. Melnyk, I.V. Melnyk, and B.A. Tugay, "Model of control of glow discharge electron gun current for microelectronics production applications," *Proceedings of SPIE. Sixth International Conference on "Material Science and Material Properties for Infrared Optoelectronics"*, vol. 5065, pp. 64–76, 2003. doi: https://doi.org/10.1117/12.502174
40. I.V. Melnyk, S.B. Tugay, "Analytical calculations of anode plasma position in high-voltage discharge range in case of auxiliary discharge firing," *Radioelectronic and Communication Systems*, vol. 55(11), pp. 50–59. 2012. doi: https://doi.org/10.3103/S0735272712110064
41. I.V. Melnyk, "Estimating of current rise time of glow discharge in triode electrode system in case of control pulsing," *Radioelectronic and Communication Systems*, vol. 56, no. 12, pp. 51–61, 2017. doi: 10.3103/S0735272713120066

42. S.V. Denbnovetskiy, I.V. Melnyk, V.G. Melnyk, B.A. Tugai, and S.B. Tuhay, "Investigation of Emission Properties of Cold Cathodes in Triode Impulse High Voltage Glow Discharge Electron Guns," *XXXV IEEE International Scientific Conference "Electronic And Nanotechnology (ELNANO)", Conference Proceedings, Kyiv, Ukraine, April 21-24, 2015*, pp. 450–453. doi: 10.1109/ELNANO.2015.7146931
43. I.V. Melnyk, "Improving Estimation of Rising Time of High Voltage Glow Discharge Current in Triode Electrodes Systems with Taking into Account Changing of Anode Plasma Parameters," *XXXV IEEE International Scientific Conference "Electronic And Nanotechnology (ELNANO)", Conference Proceedings, Kyiv, Ukraine, April 21-24, 2015,* pp. 461–464. doi: 10.1109/ELNANO.2015.7146930
44. R.W. Hockney, J.W. Eastwood, *Computer Simulation Using Particles*. CRC Press, 1988, 540 p.
45. A.O. Luntovskyy, I.V. Melnyk, "Simulation of Technological Electron Sources with Use of Parallel Computing Methods," *XXXV IEEE International Scientific Conference "Electronic And Nanotechnology (ELNANO)", Conference Proceedings, Kyiv, Ukraine, April 21-24, 2015*, pp. 454 – 460. doi: 10.1109/ELNANO.2015.7146929
46. I. Melnyk, A. Luntovskyy, "Estimation of Energy Efficiency and Quality of Service in Cloud Realizations of Parallel Computing Algorithms for IBN," in Klymash, M., Beshley, M., Luntovskyy, A. (eds) *Future Intent-Based Networking. Lecture Notes in Electrical Engineering*, vol. 831, Springer, Cham, pp. 339–379. doi: https://doi.org/10.1007/978-3-030-92435-5_20
47. I. Melnyk, S. Tuhai, and A. Pochynok, "Interpolation of the Boundary Trajectories of Electron Beams by the Roots from Polynomic Functions of Corresponded Order," *2020 IEEE 40th International Conference on Electronics and Nanotechnology (ELNANO)*, pp. 28–33. doi: 10.1109/ELNANO50318.2020.9088786
48. I. Melnik, S. Tugay, and A. Pochynok, "Interpolation Functions for Describing the Boundary Trajectories of Electron Beams Propagated in Ionised Gas," *15-th International Conference on Advanced Trends in Radioelectronics, Telecommunications and Computer Engineering (TCSET – 2020)*, pp. 79–83. doi: 10.1109/TCSET49122.2020.235395
49. I.V. Melnyk, A.V. Pochynok, "Study of a Class of Algebraic Functions for Interpolation of Boundary Trajectories of Short-Focus Electron Beams," *System Researches and Information Technologies*, no. 3, pp. 23–39, 2020. doi: https://doi.org/10.20535/SRIT.2308-8893.2020.3.02
50. I. Melnyk, S. Tuhai, M. Skrypka, A. Pochynok, and D. Kovalchuk, "Approximation of the Boundary Trajectory of a Short-Focus Electron Beam using Third-Order Root-Polynomial Functions and Recurrent Matrixes Approach," *2023 International Conference on Information and Digital Technologies (IDT)*, Zilina, Slovakia, 2023, pp. 133–138, doi: 10.1109/IDT59031.2023.10194399
51. J.I. Etcheverry, N. Mingolo, J.J. Rocca, and O.E. Martınez, "A Simple Model of a Glow Discharge Electron Beam for Materials Processing," *IEEE Transactions on Plasma Science*, vol. 25, no. 3, pp. 427–432, June, 1997. doi: 10.1109/27.597256
52. G.M. Phillips, *Interpolation and Approximation by Polynomials*. Springer, 2023, 312 p. Available: http://bayanbox.ir/view/2518803974255898294/George-M.-Phillips-Interpolation-and-Approximation-by-Polynomials-Springer-2003.pdf
53. N. Draper, H. Smith, *Applied Regression Analysis*; 3 Edition. Wiley Series, 1998, 706 p. Available: https://www.wiley.com/en-us/Applied+Regression+Analysis,+3rd+Edition-p-9780471170822
54. C. Mohan, K. Deep, *Optimization Techniques*. New Age Science, 2009, 628 p. Available: https://www.amazon.com/Optimization-Techniques-C-Mohan/dp/ 1906574219
55. M.K. Jain, S.R.K. Iengar, and R.K. Jain, *Numerical Methods for Scientific & Engineering Computation*. New Age International Pvt. Ltd., 2010, 733 p. Available: https://www.google.com.ua/url?sa=t&rct=j&q=&esrc=s&source=web&cd=&ved=2ahUKEwippcuT7rX8AhUhlYsKHRfBCG0QFnoECEsQAQ&url=https%3A%2F%2Fwww.researchgate.net%2Fprofile%2FAbiodun_Opanuga%2Fpost%2Fhow_can_solve_a_non_linear_PDE_using_numerical_method%2Fattachment%2F59d61f7279197b807797de30%2FAS%253A284742038638596%25401444899200343%2Fdownload%2FNumerical%2BMethods.pdf&usg=AOvVaw0MjNl3K877lVWUWw-FPwmV
56. S.C. Chapra, R.P. Canale, *Numerical Methods for Engineers*; 7th Edition. McGraw Hill, 2014, 992 p. Available: https://www.amazon.com/Numerical-Methods-Engineers-Steven-Chapra/dp/007339792X

57. E. Wentzel, L. Ovcharov, *Applied Problems of Probability Theory*. Mir, 1998, 432 p. Available: https://mirtitles.org/2022/06/03/applied-problems-in-probability-theory-wentzel-ovcharov/
58. J.A. Gubner, *Probability and Random Processes for Electrical and Computer Engineers*. UK, Cambridge: Cambridge University Press, 2006. Available: http:// www.amazon.com/Probability-Processes-Electrical-Computer-Engineers/dp/ 0521864704
59. M. Lutz, *Learning Python*; 5th Edition. O'Reilly, 2013, 1643 p.
60. W. McKinney, *Python for Data Analysis: Data Wrangling with Pandas, NumPy, and Jupyter*; 3rd Edition. O'Reilly Media, 2023, 579 p.

Received 11.11.2023

INFORMATION ON THE ARTICLE

Igor V. Melnyk, ORCID: 0000-0003-0220-0615, National Technical University of Ukraine "Igor Sikorsky Kyiv Polytechnic Institute", Ukraine, e-mail: imelnik@phbme.kpi.ua

Alina V. Pochynok, ORCID: 0000-0001-9531-7593, Research Institute of Electronics and Microsystem Technology of the National Technical University of Ukraine "Igor Sikorsky Kyiv Polytechnic Institute", Ukraine, e-mail: alina_pochynok@yahoo.com

Mykhailo Yu. Skrypka, ORCID: 0009-0006-7142-5569, National Technical University of Ukraine "Igor Sikorsky Kyiv Polytechnic Institute", Ukraine, e-mail: scientetik@gmail.com

УДОСКОНАЛЕНИЙ МЕТОД ІНТЕРПОЛЯЦІЇ ГРАНИЧНИХ ТРАЄКТОРІЙ КОРОТКОФОКУСНИХ ЕЛЕКТРОННИХ ПУЧКІВ ЗА ДОПОМОГОЮ КОРЕНЕВИХ ПОЛІНОМІАЛЬНИХ ФУНКЦІЙ ВИЩОГО ПОРЯДКУ ТА ЙОГО ПОРІВНЯЛЬНЕ ДОСЛІДЖЕННЯ / І.В. Мельник, А.В. Починок, М.Ю. Скрипка

Анотація. Розглянуто та обговорено узагальнене порівняння трьох сучасних, нових методів оцінювання граничної траєкторії електронних пучків, що поширюються в іонізованому газі, включаючи інтерполяцію нижчого порядку, самоузгоджену інтерполяцію та екстраполяцію, а також інтерполяцію вищого порядку. Усі оцінки відповідних похибок були проведені відносно числового розв'язування системи алгебра-диференціальних рівнянь, що описують граничну траєкторію електронного пучка. Через виконаний аналіз показано та доведено, що інтерполяція нижчого порядку зазвичай дає мінімальне значення середньої похибки, використання методу самоузгодженої інтерполяції та екстраполяції дає мінімальну похибку щодо оцінки фокальних параметрів електронного променя, а інтерполяція вищого порядку може бути використана для отримання рівномірного значення похибки на всьому інтервалі інтерполяції. Усі результати оцінювання похибок отримано з використанням оригінального комп'ютерного програмного забезпечення, створеного засобами мови програмування Python.

Ключові слова: інтерполяція, екстраполяція, інтерполяція нижчого порядку, інтерполяція вищого порядку, коренево-поліноміальна функція, яружна функція, середня похибка, електронний пучок, гранична траєкторія, високовольтний тліючий розряд, електронно-променеві технології.